Showa Univ J Med Sci **29**(3), 297～306, September 2017

Original

Image Analysis of Magnifying Endoscopy for Differentiation between Early Gastric Cancers and Gastric Erosions

Shotaro HANAMURA*, Kuniyo GOMI, Masatsugu NAGAHAMA
and Hiroshi TAKAHASHI

Abstract: The primary goal of upper gastrointestinal endoscopy is the detection of early gastric cancers, although diagnosing small gastric cancers remains difficult. Narrow-band imaging with magnifying endoscopy (NBI-ME) is a recently developed advanced endoscopic imaging technology recommended for the accurate diagnosis of gastric cancer; however, reports of NBI-ME image analysis are still scarce. This study aimed to accurately diagnose early gastric cancers based on NBI-ME findings. We compared NBI-ME image differences between small early gastric cancers and gastric erosions using computerized image analysis. We retrospectively examined 94 lesions of early gastric cancers that were treated by endoscopic submucosal dissection (ESD) from January 2011 to March 2014 in our institution and 65 lesions of erosion diagnosed by biopsy as controls. We used "ProStudy® ＜Olympus＞" as the image analysis software and compared the differences. The microvascular pattern of early gastric cancers was characterized by a larger vascular area, a more complicated depiction region, more vascular endpoints and points of intersection, and greater length and size, compared to gastric erosions. We found no differences in vascular structure between the cancers and erosions by normal endoscopy. This finding confirms the superiority of image analysis in the diagnosis of early gastric cancer. NBI-ME image analysis is a promising approach for accurate and simple diagnosis of early gastric cancers.

Key words: gastric cancer, image analysis

Objective

The primary goal of upper gastrointestinal endoscopy is the detection of early gastric cancers. Narrow-band imaging with magnifying endoscopy (NBI-ME) is a recently developed and advanced endoscopic imaging technology that can clearly visualize microvascular and microsurface patterns and has been recommended for the accurate diagnosis of gastric cancers[1, 2].

Unlike other gastrointestinal tract tumors, gastric cancers can occur within a variety of background conditions such as atrophic gastritis, metaplasia, and inflammation. In such cases, the affected background mucosa can make it difficult to accurately classify the early gastric cancer by NBI-ME[3]. This is because certain morphological features of the mucosa believed to be

Department of Gastroenterology, Showa University Fujigaoka Hospital, 1-30 Fujigaoka, Aoba-ku, Yokohama 227-8501, Japan.
* To whom corresponding should be addressed.

indicative of malignancies, such as the abrupt ending of a fold, encroachment of the border, and an irregularly shaped depression side, are difficult to assess for minute gastric cancers, making qualitative diagnosis difficult. Indeed, successful diagnosis requires a minimum lesion diameter of 3 mm[4]. Various descriptions have been used to characterize the microvascular pattern of gastric cancers in the literature; however, few of these have involved NBI-ME image analysis. Thus, it remains difficult to differentiate between early gastric cancers and gastric erosions based solely on endoscopic findings, particularly for minute gastric cancers.

On the other hand, opportunities to perform endoscopy for a patient taking antithrombotic drugs have been increasing because of the increasing use of antithrombotic drug treatments. In cases where a patient takes multiple antithrombotic drugs and the decision to discontinue treatment is difficult, screening examinations without biopsy are required, and assessing the need for re-examination for the purpose of biopsy must be performed using endoscopy.

The objective of this study was to assess the utility of NBI-ME image analysis for the accurate diagnosis of early gastric cancers.

Methods

We retrospectively examined 94 early gastric cancers that were treated by endoscopic submucosal dissection from January 2011 to March 2014 in our institution, and 65 erosions with irregular microvascular patterns that were diagnosed by biopsy as controls. In the early gastric cancer group, there were 20 lesions ≤5 mm along their greatest dimension, 38＞5 mm and ≤10 mm, 25＞10 mm and ≤20 mm, and 11＞20 mm. Histopathological analysis diagnosed 79 cancers as tub1, 5 as tub2, and 10 as tub1＋tub2. With respect to invasion depth, 84 were mucosal (m) and 10 were submucosal (sm).

Initially, we set a 128×128 pixel region from concavity with a microvascular pattern as the "area of interest" on NBI-ME images in all cases. Fig. 1 shows the area of interest on the NBI-ME image of a gastric cancer, and Fig. 2 shows the area of interest for a gastric erosion. We used ProStudy®＜Olympus＞ image analysis software and digitized images using various parameters. Eight items were set as parameters for image analysis (Table 1).

We divided the analysis results into two groups: gastric cancers and gastric erosions. The t-test was used to assess the significance of the parameters. In addition, we compared early gastric cancers ≤10 mm and erosions.

Results

Comparison between early gastric cancers and gastric erosions

The means, standard errors, and minimums and maximums of each parameter of whole early gastric cancers and erosions are detailed in Table 2, with t-test results for the parameters listed in Table 3. Differences at a significance level of 1% were detected in the vascular area ratio, fractal dimension, number of vascular endpoints, number of vascular crossings, average of the vascular length, total blood vessel length, and number of vascular picture elements / total blood vessel length (vascular thickness) between early gastric cancers and gastric erosions. There were

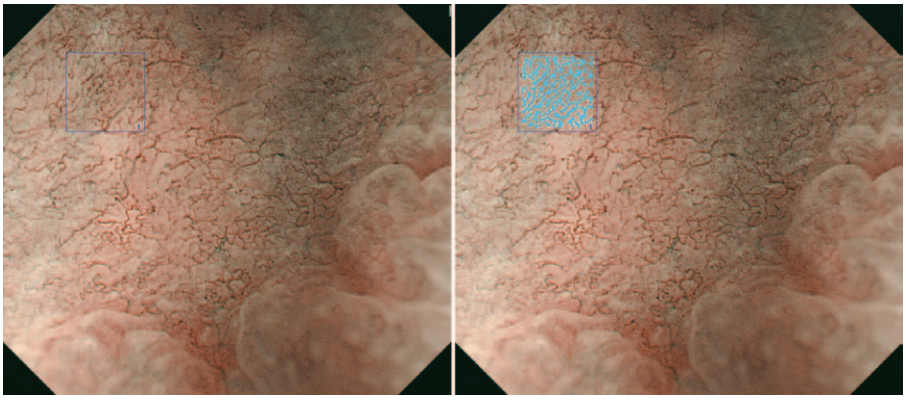

Fig. 1. NBI magnifying endoscopic image of an early gastric cancer and setting of the area of interest.

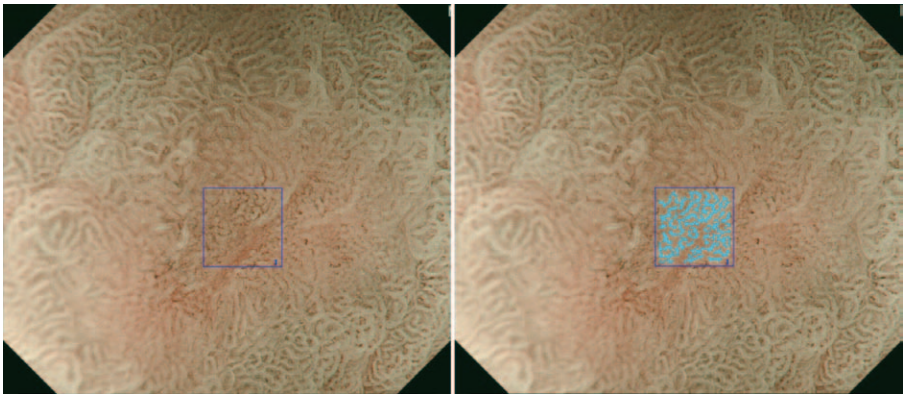

Fig. 2. NBI magnifying endoscopic image of a gastric erosion and setting of the area of interest.

Table 1. Parameters used in image analysis

① Vascular area ratio : ratio of the vascular area to the area of interest. Because this is a ratio, it is a feature that does not depend on the scan distance.
② Fractal dimension : mean of the vascular fractal dimension in the area of interest. This feature expresses the complexity of the depicted region.
③ Number of vascular endpoints : total number of vascular endpoints in the area of interest.
④ Number of vascular crossings : total number of vascular points of intersection in the area of interest.
⑤ Number of depicted blood vessels : Vascular total number in the area of interest.
⑥ Average vascular length : mean vascular length in the area of interest.
⑦ Total blood vessel length : total vascular length in the area of interest.
Total blood vessel length = Average vascular length × number of depicted blood vessels.
⑧ Number of vascular picture elements / total blood vessel length : This feature reflects the vascular thickness.

Table 2. Analysis results of all early gastric cancers and erosions

	Gastric cancer (Mean ± standard error)	Gastric cancer (minimum / maximum)	Gastric erosion (Mean ± standard error)	Gastric erosion (minimum / maximum)
Vascular area ratio	0.301 ± 0.005	0.173 / 0.408	0.246 ± 0.012	0.028 / 0.414
Fractal dimension	1.625 ± 0.006	1.478 / 1.728	1.537 ± 0.019	1.066 / 1.725
Number of vascular endpoints	24.809 ± 0.912	46.000 / 104.000	66.215 ± 2.177	19.000 / 96.000
Number of vascular crossings	50.564 ± 2.334	11.000 / 130.000	30.215 ± 2.427	1.000 / 68.000
Number of depicted blood vessels	24.404 ± 0.898	7.000 / 50.000	26.569 ± 1.000	9.000 / 46.000
Average vascular length	52.674 ± 3.615	11.200 / 229.286	31.481 ± 2.390	9.083 / 113.909
Number of vascular picture elements	4921.843 ± 81.120	3359.000 / 6574.000	3963.569 ± 194.271	449.000 / 6679.000
Total blood vessel length	1223.648 ± 21.473	720.966 / 1719.687	941.003 ± 41.615	140.974 / 1391.033
Number of vascular picture elements / total blood vessel length	3.975 ± 0.026	3.573 / 5.185	4.132 ± 0.056	3.176 / 5.694

Table 3. Results of t tests for all early gastric cancers and erosions

	t value	p value
Vascular area ratio	$\|T\| = 4.631 > t88\ (0.0005)$	$p < 0.001$
Fractal dimension	$\|T\| = 5.030 > t76\ (0.0005)$	$p < 0.001$
Number of vascular endpoints	$\|T\| = 4.082 > t100\ (0.0005)$	$p < 0.001$
Number of vascular crossings	$\|T\| = 5.885 > t149\ (0.0005)$	$p < 0.001$
Number of depicted blood vessels	$\|T\| = 1.279 \leq t146\ (0.025)$	n.s.
Average vascular length	$\|T\| = 4.431 < t150\ (0.0005)$	$p < 0.001$
Number of vascular picture elements	$\|T\| = 5.014 > t86\ (0.0005)$	$p < 0.001$
Total blood vessel length	$\|T\| = 6.550 > t98\ (0.0005)$	$p < 0.001$
Number of vascular picture elements / total blood vessel length	$\|T\| = 2.781 > t92\ (0.005)$	$p < 0.01$

no significant differences between the m and sm groups for any of the parameters.

Comparison between early gastric cancers with lesion diameters ≤10 mm and gastric erosions

The means, standard errors, and minimums and maximums of each parameter are detailed in Table 4, with t-test results listed in Table 5. Differences at the 1% level of significance were apparent in the vascular area ratio, fractal dimension, number of vascular endpoints, number

Table 4. Analysis results of ≤10-mm gastric cancers and erosions

	Gastric cancer (< 10 mm) (Mean ± standard error)	Gastric cancer (< 10 mm) (minimum / maximum)	Gastric erosion (Mean ± standard error)	Gastric erosion (minimum / maximum)
Vascular area ratio	0.293 ± 0.006	0.173 / 0.370	0.246 ± 0.012	0.028 / 0.414
Fractal dimension	1.616 ± 0.007	1.478 / 1.699	1.537 ± 0.019	1.066 / 1.725
Number of vascular endpoints	78.724 ± 1.359	60.000 / 104.000	66.215 ± 2.177	19.000 / 96.000
Number of vascular crossings	46.000 ± 2.525	11.000 / 78.000	30.215 ± 2.427	1.000 / 68.000
Number of depicted blood vessels	27.276 ± 1.114	8.000 / 50.000	26.569 ± 1.000	9.000 / 46.000
Average vascular length	44.198 ± 3.386	11.200 / 144.875	31.481 ± 2.390	9.083 / 113.909
Number of vascular picture elements	4720.914 ± 104.558	3359.000 / 5969.000	3963.569 ± 194.271	449.000 / 6679.000
Total blood vessel length	1195.889 ± 26.016	720.966 / 1513.412	941.003 ± 41.615	140.974 / 1391.033
Number of vascular picture elements / total blood vessel length	3.950 ± 0.028	3.632 / 4.866	4.132 ± 0.056	3.176 / 5.694

Table 5. Results of t tests of ≤10-mm gastric cancers and erosions

	t value	p value
Vascular area ratio	$\|T\| = 3.283 > t97\ (0.005)$	$p < 0.01$
Fractal dimension	$\|T\| = 3.686 > t82\ (0.0005)$	$p < 0.001$
Number of vascular endpoints	$\|T\| = 4.740 > t106\ (0.0005)$	$p < 0.001$
Number of vascular crossings	$\|T\| = 4.502 > t120\ (0.005)$	$p < 0.001$
Number of depicted blood vessels	$\|T\| = 0.467 \leq t117\ (0.025)$	n.s.
Average vascular length	$\|T\| = 3.119 > t105\ (0.005)$	$p < 0.01$
Number of vascular picture elements	$\|T\| = 3.319 > t97\ (0.005)$	$p < 0.01$
Total blood vessel length	$\|T\| = 5.052 > t106\ (0.0005)$	$p < 0.001$
Number of vascular picture elements / total blood vessel length	$\|T\| = 2.780 > t94\ (0.005)$	$p < 0.01$

of vascular crossings, average vascular length, total blood vessel length, and number of vascular picture elements / total blood vessel length (vascular thickness).

Comparison between early gastric cancers with lesion diameters ≤5 mm and gastric erosions

The means, standard errors, and minimums and maximums of each parameter are detailed in

Table 6. Analysis results of ≤5-mm gastric cancers and erosions

	Gastric cancer (< 10 mm) (Mean ± standard error)	Gastric cancer (< 10 mm) (minimum / maximum)	Gastric erosion (Mean ± standard error)	Gastric erosion (minimum / maximum)
Vascular area ratio	0.282 ± 0.017	0.173 / 0.369	0.246 ± 0.012	0.028 / 0.414
Fractal dimension	1.595 ± 0.024	1.478 / 1.699	1.537 ± 0.019	1.066 / 1.725
Number of vascular endpoints	77.450 ± 3.174	60.000 / 104.000	66.215 ± 2.177	19.000 / 96.000
Number of vascular crossings	42.800 ± 5.083	11.000 / 78.000	30.215 ± 2.427	1.000 / 68.000
Number of depicted blood vessels	27.700 ± 2.022	12.000 / 48.000	26.569 ± 1.000	9.000 / 46.000
Average vascular length	41.585 ± 5.743	11.200 / 107.750	31.481 ± 2.390	9.083 / 113.909
Number of vascular picture elements	4547.050 ± 268.122	3359.000 / 5969.000	3963.569 ± 194.271	449.000 / 6679.000
Total blood vessel length	1152.953 ± 65.856	720.966 / 1513.412	941.003 ± 41.615	140.974 / 1391.033
Number of vascular picture elements / total blood vessel length	3.941 ± 0.038	3.685 / 4.241	4.132 ± 0.056	3.176 / 5.694

Table 7. Results of t tests of ≤5-mm gastric cancers and erosions

	t value	p value
Vascular area ratio	$\|T\| = 1.483 \leq t43\ (0.025)$	n.s.
Fractal dimension	$\|T\| = 1.525 \leq t49\ (0.025)$	n.s.
Number of vascular endpoints	$\|T\| = 2.544 > t40\ (0.025)$	$p < 0.05$
Number of vascular crossings	$\|T\| = 2.313 > t30\ (0.025)$	$p < 0.05$
Number of depicted blood vessels	$\|T\| = 0.454 \leq t30\ (0.025)$	n.s.
Average vascular length	$\|T\| = 1.828 \leq t27\ (0.025)$	n.s.
Number of vascular picture elements	$\|T\| = 1.506 \leq t43\ (0.025)$	n.s.
Total blood vessel length	$\|T\| = 2.520 > t37\ (0.025)$	$p < 0.05$
Number of vascular picture elements / total blood vessel length	$\|T\| = 1.785 \leq t74\ (0.025)$	n.s.

Table 6, and the t-test results are shown in Table 7. There were differences at the 5% level of significance in number of vascular endpoints, number of vascular crossings, and total blood vessel length.

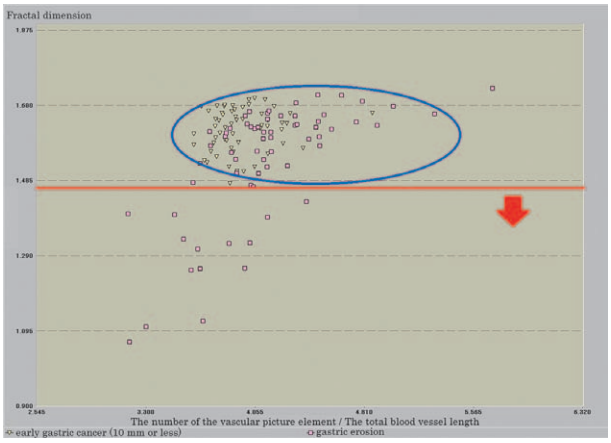

Fig. 3. Scatter diagram of ≤10-mm early gastric cancers and gastric erosions with the number of vascular picture elements / total blood vessel length (a feature quantity that reflects vascular thickness) and fractal dimension representing the axes. We consider that the cases under the red line did not require biopsy for the diagnosis of early gastric cancer. In contrast, the cases located within the blue oval were thought to require a biopsy for positive identification.

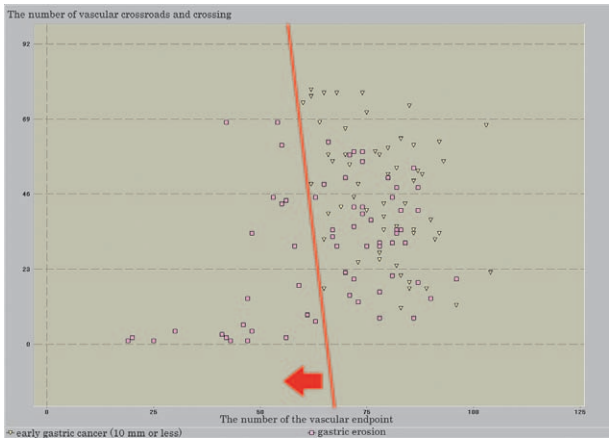

Fig. 4. Scatter diagram of the ≤10-mm early gastric cancers and gastric erosions with the number of vascular endpoints and vascular crossings of the parameters representing the axes. We consider that the cases under the red line did not require biopsy for the diagnosis of early gastric cancer.

Scatter diagram of the parameters that showed significant differences between early gastric cancers and gastric erosions

A scatter diagram was created showing the number of blood vessel picture elements / total blood vessel length (quantity that potentially reflects vascular thickness) and fractal dimension along both axes using the parameters that showed a significant difference between early gastric cancers with diameters ≤10 mm and gastric erosions (Fig. 3). Clinical applications were also examined. Similarly, we created a scatter plot with vascular endpoints and vascular crossings along both axes (Fig. 4). The dispersal of both groups showed deflection, but a region where the distribution of both groups of data clustered was also found.

Discussion

Our examination of all early gastric cancers and gastric erosions in this study revealed the microvascular pattern of the early gastric cancers to have a larger vascular area, more complicated depiction region, more vascular endpoints and vascular points of intersection, and greater length and size than those in the microvascular pattern of the gastric erosions. The microvascular patterns of early gastric cancers and gastric erosions for which the differential diagnosis was difficult were significantly different on the NBI-ME images digitized in the image analysis. The report of Araki *et al* in which analysis was performed by estimating morphological differences in the microvessels between early gastric cancers and backgrounds using a skeleton pixel and picture element that extracted a vascular central ray similar to a frame showed that the micro-

vasculature of early gastric cancers had more connection, terminal, and branching points than the background[5]. These findings are consistent with ours, which showed significant differences of vascular endpoints and vascular points of intersection between early gastric cancers and gastric erosions.

Our examination of the early gastric cancers with diameters ≤10 mm and gastric erosions showed significant differences in parameters similar to those described above. Specifically, the microvascular pattern of this early gastric cancer subset had a larger vascular area, more complicated depiction region, more vascular endpoints and vascular points of intersection, and greater length and size than those of the gastric erosions. Digitization of the NBI-ME images in the image analysis thus revealed significant differences between small early gastric cancers and gastric erosions.

Comparison of the microvascular patterns of early gastric cancers and gastric erosions by NBI-ME revealed significant differences across various parameters. We also found a region in these images where the distributions of data sets for parameters clustered on a scatter diagram, although it was difficult to set a clear boundary value. Nevertheless, this clustering suggested that the scatter diagram could be used in differential diagnosis.

In the screening examinations performed only by observations without biopsies for cases in which it was difficult to decide if the administration of anticoagulants should be discontinued, we found that the positions in the scatter diagram of the obtained data could be useful for diagnosis when reviewing endoscopic re-examination results for the purpose of biopsy. Indeed, the scatter diagram analyses represented in Fig. 3 indicated that those cases exhibiting lower than the minimum fractal dimension did not require biopsy for the diagnosis of early gastric cancer. In contrast, the cases located within the blue oval were thought to require a biopsy for positive identification. From the scatter diagram represented in Fig. 4, we think that the cases at positions lower than the line linking the minimum "number of vascular crossings" to "number of vascular endpoints" of early gastric cancers did not require biopsy for diagnosis.

Our evaluation of the NBI-ME in real time suggested that image analysis should be used only after endoscopic examination to aid in judging the need for re-examination, because it is necessary for an endoscopic enforcer to set the area of interest.

Gastric erosions can exhibit network patterns similar to well differentiated adenocarcinoma, which may make differentiation between gastric erosions and gastric cancers difficult[6]. To this end, Yao *et al*[7] found that NBI-ME showed superior sensitivity and diagnosis rate compared to normal endoscopy, and that four out of eight patients were misdiagnosed because of the magnification limit of the endoscope. Furthermore, Fujiwara *et al*[8] reported a higher capacity for accurate diagnosis with NBI-ME compared to chromoendoscopy. Their study examined why non-cancerous lesion might be incorrectly diagnosed as cancers using NBI-ME, and found that minor irregularities in the microvascular pattern could prompt a cancer diagnosis, that the magnified endoscopic images were not taken in the on-face view, and that a low magnifying ratio also contributed to the error.

Finally, Uchida *et al*[9] reported that mucosal border diagnosis by NBI-ME revealed that the

epithelial structure in lesions was similar to that in the background mucosa, making it difficult to diagnose based only on structure visualized by low-power observation. In support of this, we found in the present study that observing microvascular form at maximal magnification improved the endoscopic power of diagnosis. It should also be noted that observation by NBI-ME at the maximal magnification is technically difficult and requires training, but that technical acquisition is clearly desirable for better diagnostic ability.

By the increase of elderly people, endoscopic frequency increases and leads to increase of the discovery of small gastric cancers [10]. And the microvascular irregularity and expansion are relieved, because inflammation in the cancer lesion is improved by *Helicobacter pylori* eradication [11]. Aging and the spread of sanitization treatment may result in early gastric cancer diagnosis difficulty in the future, and it is thought that more careful endoscopic observation will be required.

Endoscopic diagnosis of minute gastric cancers by NBI-ME has progressed recently, and several studies including this one have shown its value ; however, examiners still require appropriate experience and expertise in endoscopic technique and diagnostics to gain the full diagnostic benefit.

In conclusion, image digitization is inherently objective, and thus this NBI-ME image analysis technology could assist diagnoses of early gastric cancer.

Acknowledgment

The authors thank Dr. K. Ukawa for his valuable comments.

Conflict of interest disclosure

The authors declare that they have no conflict of interest.

References

1) Yao K. Zoom gastroscopy: magnifying endoscopy in the stomach. Tokyo: Nihon Medical Center; 2009. (in Japanese).
2) Oyama T. Endoscopic diagnosis of gastric adenocarcinoma for ESD. Tokyo: Nankodo; 2010. (in Japanese).
3) Fujisaki J, Okada K, Hirasawa T, *et al*. Differential diagnosis of gastric tumors using magnifying endoscopy in the diagnosis of depressed epithelial tumors. *Stomach Intestine*. 2011;**46**:867-880. (in Japanese).
4) Takahashi H, Hirata K, Sawada S, *et al*. Endoscopic diagnosis of minute gastric cancers. *Gastroenterol Endosc*. 2011;**53**:1229-1240. (in Japanese).
5) Araki Y, Sasaki Y, Hanabata N, *et al*. Morphometry for microvessels in early gastric cancer by narrow band imaging-equipped magnifying endoscopy. *Dig Endosc*. 2011;**23**:233-239.
6) Fujisaki J, Saito M, Yamamoto Y, *et al*. Diagnosis of minute early gastric cancer using magnified endoscopy-especially using magnified-narrow band imaging. *Gastroenterol Endosc*. 2006;**48**:1470-1479. (in Japanese).
7) Yao K, Fujiwara S, Nagahama T, *et al*. Diagnostic performance and limitations of magnifying narrow-band imaging for the diagnosis of minute gastric cancer. *Stomach Intestine*. 2013;**48**:843-856. (in Japanese).
8) Fujiwara S, Yao K, Nagahama T, *et al*. Can we accurately diagnose minute gastric cancer (≤5 mm)? Chromoendoscopy (CE) vs magnifying endoscopy with narrow band imaging (M-NBI). *Gastric Cancer*. 2015;**18**:590-596.
9) Uchita K, Yao K, Iwasaki T, *et al*. The effect of different magnification levels on the ability to delineate margins

of early gastric cancers. *Stomach Intestine*. 2015;**50**:301–310. (in Japanese).

10) Nagai K, Tatsuta M, Matsuura N, *et al*. Changing trends in diagnosis of minute gastric cancers. *Stomach Intestine*. 2013;**48**:785–793. (in Japanese).

11) Kobayashi M, Hashimoto S, Mizuno K, *et al*. Magnifying narrow-band imaging of early gastric cancers detected after *Helicobacter pylori* eradication. *Stomach Intestine*. 2015;**50**:289–299. (in Japanese).

[Received February 16, 2017 : Accepted March 3, 2017]